Discover Oncology

Research

CD206 accelerates hepatocellular carcinoma progression by regulating the tumour immune microenvironment and increasing M2-type polarisation of tumour-associated macrophages and inflammation factor expression

Zhiyuan Mao^{1,2,3} · Yalin Han^{4,5} · Yinglin Li^{1,2} · Li Bai²

Received: 20 December 2023 / Accepted: 3 September 2024

Published online: 13 September 2024

© The Author(s) 2024

OPEN

Abstract

Objective This study aims to investigate the effect of CD206 on the progression of hepatocellular carcinoma (HCC) and the regulation of the tumour immune microenvironment.

Methods A subcutaneous mouse model of HCC was established and treated with CD206-overexpressing adenovirus by tail vein injection or CD206 antibody C068C2 by intratumoral injection. The hepatocarcinoma-bearing mice were divided into four groups (IgG+ tail vein adenovirus group, IgG group, C068C2+ tail vein adenovirus group and C068C2 group) to observe the changes in tumour weight and volume with different expression levels of CD206. The proportion of M2-type tumour-associated macrophages (TAMs) was detected by flow cytometry and immunofluorescence. The apoptosis of tumour cells was detected using terminal deoxynucleotidyl transferase dUTP nick-end labelling (TUNEL) staining, and inflammatory factors in serum and tissues were detected using the ENZYME-LINKED IMMUNOSORBENT ASSAY.

Results Compared with the mice with low CD206 expression, the hepatocarcinoma-bearing mice with high CD206 expression in HCC exhibited faster tumour growth and more aggressive progression. Flow cytometry and immunofluorescence staining revealed that the expression level of CD206-positive M2-type TAMs was highest in the IgG+ adenovirus group and lowest in the C068C2 group (p < 0.001). Compared with the IgG+ adenovirus group, the proportion of TUNEL-positive cells in tumour cells was significantly reduced in the C068C2 group. The IgG+ adenovirus group had the highest concentrations of transforming growth factor- β (TGF- β) and interleukin 6 (IL-6) in both serum and tumour tissues. Conclusion The overexpression of CD206 accelerates the progression of HCC and changes the tumour immune microenvironment. The high expression of CD206 in HCC increases the M2-type polarisation of TAMs and induces the expression of both TGF- β and IL-6 in tumour tissues and serum, thereby promoting HCC progression.

Keywords Hepatocellular carcinoma \cdot Tumour-associated macrophages \cdot Immune microenvironment \cdot Inflammatory factors \cdot CD206

Zhiyuan Mao and Yalin Han contributed equally to this study.

[☑] Li Bai, baili_li885@163.com | ¹Department of Oncology, Air Force Medical Center of Chinese PLA, Beijing 100142, China. ²Department of Oncology, The First Medical Center, Chinese PLA General Hospital, No. 28 Fuxing Road, Haidian District, Beijing 100853, China. ³Department of Oncology, Medical School of Chinese PLA, Beijing 100853, China. ⁴Department of Oncology, PLA Rocket Force Characteristic Medical Centre, Beijing 100088, China. ⁵Department of General Surgery, The First Medical Centre, Chinese PLA General Hospital, Beijing 100853, China.



Discover Oncology (2024) 15:439

https://doi.org/10.1007/s12672-024-01309-1



1 Introduction

Hepatocellular carcinoma (HCC) is the fifth most common malignancy and the third leading cause of cancer-related deaths worldwide [1]. Despite great improvements in the diagnosis and treatment of HCC, the clinical outcomes of patients with this disease remain poor. High invasiveness, recurrence and metastasis are the main reasons for the poor prognosis of patients with HCC [2]. Such patients are usually diagnosed at an advanced stage, which leads to unresectability and limited treatment options. Resistance to chemotherapy remains the main reason for treatment failure [3].

The tumour microenvironment (TME) is composed of cancer cells, stromal cells, immune cells, cytokines, etc. [4, 5]. The crosstalk between HCC and the TME can provide a microenvironment that is favourable for tumour growth and progression. Tumour-associated macrophages (TAMs) are also involved in TMEs and play an important role, mainly in tumour formation, development, invasion and metastasis. Tumour microenvironments can be divided into M1 and M2 phenotypes. M1-type TAMs account for the majority of TAMs in the early stages of tumours and slowly change to M2-type TAMs with tumour progression [6]. Many studies have shown that M2-type TAMs can accelerate cancer cell proliferation, invasion and metastasis, promote angiogenesis and immune escape [7, 8], be significantly involved with tumour progression and treatment resistance and shorten the survival time of patients [9, 10]. M1-type TAMs have been proven to inhibit tumour growth, mainly via the immune response and the recognition and killing of tumour cells [11, 12]. M1-type and M2-type TAMs represent dynamic changes in the TME and can transform into each other by changing the TME, thereby affecting the polarisation of TAMs [12]. Clinical data have shown that the higher the number of M2-type TAMs, the worse the prognosis of patients with cancer; additionally, there is a certain relationship between M2-type TAMs and treatment resistance, which suggests that M2-type TAMs can be used as prognostic biomarkers and therapeutic targets [12–14].

At present, the main mechanism for drugs targeting M2-type TAMs acts to clear them from the TME or block their inhibitory function [15]. Thus, comprehensively studying the characteristics and regulation of TAMs may elucidate their correlation with the prognosis and therapeutic response of patients with HCC.

CD206, a mannose receptor, belongs to the calcium-dependent type-I transmembrane protein receptor. It is widely distributed in macrophages in tissues, such as the paracortex of lymph nodes, the cortex of the thymus and the red pulp of the spleen, and it is the most specific marker on the surface of M2-type TAMs [16]. Mannose receptors can recognise a variety of sugar molecules in the pathogen cell wall or cell surface and participate in and regulate the body's immune defence via receptor-mediated phagocytosis and endocytosis [17]. In previous studies, the density of CD206-positive TAMs was found to be an independent predictor of lower progression-free survival (PFS) in breast cancer in different populations [13], and the expression of CD206 in TAMs is related to the differentiation, depth of invasion, vascular tumour thrombus and nerve invasion of colon cancer. Another study showed that lung cancer cells can induce M1-type TAMs to polarise to M2-type TAMs with positive CD206 expression via THP-1 and stimulate the production of a variety of cytokines [14]. However, it is unknown whether regulating the expression levels of CD206 in HCC is related to the progression of HCC, and the involvement of inflammation factors and the M2-type polarisation of TAMs have not been clarified.

This study focused on the crosstalk between TAMs and HCC via CD206 and hypothesised that the tumour immune microenvironment could be reprogrammed using different levels of CD206 in HCC. Based on this, CD206 can regulate the expression levels of inflammatory factors and drive the differentiation of TAM cells, increase the proportion of M2-type TAMs and promote HCC progression.

Herein, CD206 was used as the marker of M2-type polarised TAMs. A mouse model was established with subcutaneous tumours, and the mice were treated with CD206-overexpressing adenovirus or CD206 antibody C068C2 to investigate the effect of CD206 on HCC progression. In this study, the authors aimed to investigate tumour growth, tumour cell apoptosis, the proportion of M2-type TAMs and the inflammation factors of transforming growth factor- β (TGF-β) and interleukin 6 (IL-6) in serum and tumour tissues with different levels of CD206 treatment.

2 Materials and methods

2.1 Animals

Twenty 8-week-old female nude mice were used in this study, all of which were purchased from Beijing Weitong Lihua Laboratory Animal Technology Co., Ltd. The nude mice were housed according to the specific pathogen-free



animal husbandry requirements. The animals were fed ad libitum and had free access to water. Their drinking water was changed daily, and the water bottles for holding drinking water were autoclaved daily. The cages and accessories were cleaned, disinfected and replaced regularly and were autoclaved and used in a barrier environment. All experimental procedures involving the animals were performed in accordance with the 3R (replacement, reduction and refinement) principles and the guidelines of the *National and Beijing Experimental Animal Welfare Ethics*.

2.2 Cell culture

The HepG2 cell line was purchased from the cell bank of the Shanghai Chinese Academy of Sciences. Eagle's minimum essential medium and Earle's Balanced Salts (HyClone) containing 10% foetal bovine serum (FBS; HyClone) and 1% non-essential amino acids (HyClone) were used for cell culture in a constant-temperature incubator at 37 °C and 5% CO₂. The HepG2 cells were passaged every 2–3 days with 0.5 mg/ml trypsin (1:250) and 0.53 mM ethylenediaminetetraacetic acid.

2.3 Construction of adenovirus plasmid and preparation of adenovirus

Reverse transcription of total RNA was used to extract cDNA from cells using a reverse transcription kit. According to the CD206 gene's known complete mRNA sequence, mouse CD206 cloning primers were designed using the Primer Premier 5.0 software for plasmid construction. The primer information was as follows: F: CGCAAATGGGCGTAGGCGTG; R: GGAAAGGACAGTGGAGTG. Recombinant adenovirus overexpressing CD206 was packaged and purified using Pure Era Biotechnology (Guangzhou, China). Finally, recombinant adenovirus with a titre of 1.2×10^{11} pfu/ml was collected.

2.4 Construction of subcutaneous mouse model of hepatocellular carcinoma

Xenotransplantation was performed in nude mice. The authors used CD206 overexpressing adenoviruses as a backup, then subcutaneously injected HepG2 cell lines into the nude mice to construct a mouse subcutaneous tumour-bearing model. On this basis, CD206 overexpression adenovirus was injected into the tail vein, and C068C2 was injected into the tumour to achieve different concentrations of CD206. The subcutaneous mouse model was divided into four groups (n = 5 each) [18]: (1) mice in the lgG+adenovirus group were treated with CD206-overexpressing adenovirus by tail vein injection and IgG antibody by intratumoral injection; (2) mice in the IgG group were treated with IgG antibody by intratumoral injection only; (3) mice in the C068C2+ tail vein adenovirus group were treated with CD206-overexpressing adenovirus by tail vein injection and C068C2 by intratumoral injection; and (4) mice in the C068C2 group were treated with C068C2 by intratumoral injection only. The HepG2 cells in the logarithmic phase were digested and centrifuged, and the resulting cells (approximately 5×10^6) were dissolved in 0.1 ml Dulbecco's modified eagle medium and mixed thoroughly. The dorsal skin of the mice was fully disinfected with 75% medical alcohol, and 0.2 ml of cell solution was subcutaneously injected into each nude mouse. At about 2 weeks after inoculation, masses began to appear subcutaneously in the nude mice. Adenovirus (40 μ l; viral titre: 1.2×10^{11} pfu/ml) was injected into the tail vein, and C068C2 (20 μ l in 5 points; concentration: 0.25 μg/100 μl) was injected intratumorally once a week. The tumour volume was measured until the end point of observation (60 days), and the tumour was weighed after the mice were euthanised. The size of the tumour was measured with vernier callipers, and the length (L) and width (W) of the tumour were recorded. The volume (V) was $(L \times W^2) \times 0.5$.

Because no functional antibody to CD206 is currently marketed, C068C2 was selected as an antibody to reduce CD206 levels in vivo and was experimentally found to have no effect on the survival of the mice. Sixty days after the subcutaneous inoculation of tumour cells (the end point of observation), 0.1 ml of peripheral blood was collected from the tail vein of the mice. Labelling was performed for the subsequent experiments. The mice were euthanised by dislocation and pulp breaking. At this time, subcutaneous tumour formations were isolated from the mice, tumour volumes were measured, tumours were weighed, and labelling was performed for the subsequent experiments.

2.5 Flow cytometry

After the tumour tissue was digested into single cells, $100 \mu l$ of cell suspension was placed into an EP tube. After the antibody was diluted 1000-fold with PBS, $1 \mu l$ was added to each tube, mixed well and incubated at room temperature in the dark for $30 \mu l$. Then, $2 \mu l$ of flow cytometry washing solution (PBS + $10 \mu l$) was added, mixed well and centrifuged



(2024) 15:439

at 300 rpm for 5 min. The supernatant was subsequently discarded. Next, 2 ml of flow cytometry wash (PBS + 1% FBS) was added and centrifuged at 300 rpm for 5 min, and the supernatant was discarded.

At the same time, a corresponding isotype control detection tube was created, and the corresponding isotype control antibody was added. The antibody information was as follows: fluorescein isothiocyanate anti-human CD68 antibody (RUO137005, BioLegend, Beijing, China); Alexa Fluor® 647 anti-human CD206 (MMR) antibody (RUO321116, Thermo, Waltham, MA, USA). Then, 2 ml of 1×Permeabilization Wash Buffer 300 was added and centrifuged for 5 min, and the supernatant was discarded. Next, 2 ml of flow cytometry washing solution (PBS + 1% FBS) was added, mixed well and centrifuged at 300 rpm for 5 min. The supernatant was subsequently discarded. Cells were resuspended by adding 0.5 ml of flow cytometry wash (PBS + 1% FBS) and were analysed on a Cytek NL-CLC3000 (Cytek Biosciences, CA, USA) system. The flow cytometry data were analysed using the FlowJo™ software.

2.6 Immunofluorescence assay

After deparaffinising the tissue sections, the PBS solution was washed three times for 5 min each. The cell membranes were ruptured using 0.2% Triton X-100 for 10 min and washed three times with PBS solution for 5 min each time. The PBS solution was discarded, and the excess solution was wiped off with filter paper. Next, the sample was dropped into a blocking solution and incubated in a humidified chamber at room temperature for 2 h. The blocking solution was subsequently discarded, the primary antibody was added at a ratio of 1:200, and the solution was left overnight at 4 °C. The wet box was removed and reheated for 30 min. Next, the primary antibody working solution was discarded, and the sample was rinsed in PBS solution three times for 5 min each time. Then, the PBS solution was discarded, the excess solution was wiped off with filter paper, and the secondary antibody working solution was added dropwise at a ratio of 1:200 (it was protected carefully from light). The temperature was set at 37 °C for incubation, which took 2 h. Following incubation, the secondary antibody working solution was removed and rinsed three times for 5 min each time with PBS solution, and the PBS solution was removed and stained with DAPI for 10 min.

The slides were mounted with an anti-fluorescence quenching mounting medium, and the results were observed and recorded under a fluorescence microscope. The information was as follows: CD68 (Ab955, Abcam, Cambridge, UK); CD206 (sc-376108, Santa Cruz, CA, USA); goat anti-rabbit IgG HampL (Alexa Fluor® 594) (ab150080, Abcam, Cambridge, UK); and mouse anti-goat IgG HampL (Alexa Fluor® 488) (ab150080, Abcam, Cambridge, UK). The DAPI-stained nuclei were blue under UV excitation, CD206-positive expression was shown as green fluorescence, and CD68-positive expression was shown as red fluorescence.

The results were interpreted by two senior attending physicians (Dechang Li and Jichun Zheng) in the pathology department of the authors' hospital based on their clinical and scientific research experience [18]. Ten high-power fields (400×, typical tumour site) were randomly selected. Grade 1: no fluorescence or very weak fluorescence; Grade 2: weak but visible fluorescence; Grade 3: bright fluorescence, yellowish green; and Grade 4: bright fluorescence, obvious bright green. Grades 1 and 2 represented low expression, and grades 3 and 4 represented high expression.

2.7 Terminal deoxynucleotidyl transferase dUTP nick-end labelling staining

Experiments were performed using a terminal deoxynucleotidyl transferase dUTP nick-end labelling (TUNEL) staining kit (At005-2, Qihai Bio, Shanghai, China). After deparaffinising the tissue sections, the PBS solution was washed three times for 5 min each time. Triton X-100 solution was added dropwise to the sections to cover the entire tissue specimen, which was kept warm and moist for 10 min. The PBS solution was fully rinsed three times for 5 min each time, and water around the tissue was removed with absorbent paper. Proteinase K solution was added dropwise to the sections to cover the entire tissue specimen, which was kept warm and moist for 30 min, and PBS solution was fully rinsed three times for 5 min each time. The labelled reaction solution was dropped so that it covered the entire tissue specimen, which was kept warm and moist for 90 min. Then, the PBS solution was rinsed thoroughly three times for 5 min each time. Next, propidium iodide (PI) staining solution was dropped onto the samples to cover the whole tissue specimen, which was kept warm and moist for 5 min, before rinsing thoroughly with PBS solution three times for 5 min each time.

The tissue sections were mounted using a prepared anti-fluorescence quenching mounting medium. The DAPI staining results showed blue nuclei under UV excitation, PI fluorescein labelling for apoptosis detection and red positive apoptotic nuclei. The results were interpreted by two senior attending physicians (Dechang Li and Jichun Zheng) in the pathology department based on previous literature [19]. The apoptosis rate was calculated, and five high-power fields (400-fold) with the highest number of apoptotic cells were selected to assess the percentage of red apoptotic nuclei in



500 tumour cells. Grade 1: ≤ 25%; Grade 2: 26%–50%; Grade 3: 51%–75%; and Grade 4: ≥ 76%. Grades 1 and 2 represented low apoptotic rates, and grades 3 and 4 represented high apoptotic rates.

2.8 Enzyme-linked immunosorbent assay

Gradient standard solutions and washing buffers were prepared while removing the ENZYME-LINKED IMMUNOSORBENT ASSAY (ELISA) kit for use. The kits used were a Mouse IL-6 ELISA Kit (RXSWSXB203049M, Ruixin Biological, Guangzhou, China) and a Mouse Transforming Growth Factor \(\beta \) ELISA Kit (RX202402M, Ruixin Biological, Guangzhou, China). After the mice were euthanised, subcutaneous tumour tissues were isolated and typical tumour sites (50 mg) were selected; then, the tissues were homogenised in PBS extraction buffer, and the supernatant was centrifuged for future use. Each well of the kit was marked respectively, divided into blanks, controls and samples, and the corresponding liquid was added. Following the addition of the respective fluids to each well, horseradish-peroxidase-labelled detection antibodies were added. Then, each well was sealed and allowed to react for 60 min at 37 °C.

After sufficient reaction, the plate was washed thoroughly five times. A substrate mixture was added to each well and allowed to react for 15 min under the same conditions. After sufficient reaction, a stop solution was added to each well to complete the process. A microplate reader was used to detect optical density (OD) values under specific conditions (within 15 min at 450 nm wavelength), and the results were recorded. According to the test results, a curve of the changes in OD value with concentration was plotted, and using the curve, the sample concentration corresponding to the OD value was calculated.

2.9 Western blot

Protein expression was detected using Western blot. Following completion of electrophoresis, transfer experiments were performed using PVDF membranes to transfer proteins from the gel to PVDF membranes. After the transfer membrane was completed, 3% BSA solution was used for blocking, and the PVDF membrane after the transfer membrane experiment was soaked in 3% BSA solution and blocked at room temperature for 30 min on a horizontal shaker. Following completion of blocking, primary antibodies were used for overnight incubation. The specific information of primary antibody was as follows: CD206:24595, CST; GAPDH: 5174, CST. After the completion of primary antibody incubation, TBST solution was used for washing three times for 10 min each wash. Following the completion of the primary antibody wash, incubation was performed using the diluted secondary antibody solution and the conditions for the secondary antibody incubation were room temperature for 30 min. Following completion of the secondary antibody incubation, the same wash was performed using TBST solution three times for 10 min each wash. After washing was completed, imaging was performed using gel imaging analysis.

2.10 Statistical analysis

A statistical analysis was performed using the SPSS 26.0 software. The measurement data from the four groups were analysed using a one-way ANOVA, and further two-by-two comparisons between groups were performed using the least significant difference t-test. The enumeration data were analysed using the χ^2 test, and further two-by-two comparisons between groups were performed using the Bonferroni test. For Bonferroni test, an adjusted p value < 0.0166 was considered statistically significant, and p < 0.05 was considered statistically significant in the remaining tests.

3 Results

3.1 Differences in CD206 expression levels in tumour tissues

The treated HCC tumour cells were injected into nude mice, and subsequent experiments were performed after tumour formation. The number of the CD206-labelled cells in tumour tissues was detected by flow cytometry. The proportions of CD206-labelled cells in the IgG+adenovirus group, IgG group, C068C2 group and C068C2+adenovirus group were significantly different (p < 0.001), with proportions of 74.47%, 67.07%, 52.57% and 45.83%, respectively. The results in Table 1 and Fig. 1A-D further showed a statistically significant difference in the proportions of CD206-labelled cells between the lgG+ adenovirus group and the other three groups, respectively (p < 0.05, p < 0.001 and p < 0.001), indicating



Table 1 Flow cytometry for CD206 differences between groups

Group	Mean	SE	F ^a	<i>p</i> value ^a	t ^b	<i>p</i> value ^b
IgG + adenovirus group	74.47	11.900	121.075	< 0.001		_
lgG group	67.07				1.656	0.050
C068C2 + adenovirus group	52.57				0.639	< 0.001
C068C2 group	45.83				1.134	< 0.001

n=5 per group

Mean: the average of the proportion of CD206 labeled cells occupying CD68 labeled cells among 5 mice in each group

a:The four-group data were analyzed using one-way ANOVA

b: Further two-by-two comparisons between groups were performed using the LSD-t test. The data in the IgG+adenovirus group was compared with the data in the three groups of IgG group, C068C2+adenovirus group and C068C2 group in pairs, respectively

that the expression level of CD206 in tumour tissue was significantly higher in the IgG+adenovirus group than in the other groups. Treatment with CD206 antibody C068C2 significantly decreased intracellular CD206 expression, indicating the efficacy of C068C2 (Fig. 1A–D).

Subsequently, the cell numbers of M2-type TAMs were further examined by flow cytometry. Macrophages were labelled using CD68, and M2-type TAMs were labelled using CD206. The results showed that in the IgG+adenovirus group, the CD206-labelled M2-type TAMs comprised the highest proportion of TAMs, and as CD206 was inhibited, the proportion of the CD206-labelled M2-type TAMs was decreased. In the C068C2 group, the CD206-labelled M2-type TAMs comprised the lowest proportion (Fig. 1A–E). Subsequently, we detected the expression of C206 in HCC clinical patient samples and found that CD206 expression was present in HCC clinical patient samples (Fig. 1F).

3.2 Differential expression of CD206 in tumour tissues detected by immunofluorescence

The expression of CD206 in tumour tissues was detected by immunofluorescence. The results (Table 2, Fig. 2A–D) showed that the expression levels of CD206 in the $\lg G + adenovirus$ group, $\lg G + adenovirus$ group, C068C2 group, and C068C2 + adenovirus group were significantly different (p < 0.05). When compared with the three other groups, the Bonferroni test only showed a statistically significant difference between the $\lg G + adenovirus$ group and the C068C2 group (p < 0.01), indicating that the expression level of CD206-labelled M2-type TAMs in tumour tissue was significantly higher in the $\lg G + adenovirus$ group than in the C068C2 group.

3.3 Effect of different expression levels of CD206 on tumour volume and growth

Adenovirus and C068C2 were injected into the tail vein and tumour regularly to measure the tumour volume; the tumour was weighed and the tumour volume and tumour weight curves drawn after the mice were euthanised (Fig. 3A–C).

There was no statistical difference in the volume of subcutaneous tumour formation after the subcutaneous injection of HepG2 cells. The tumour volume was measured every 5 days from day 20 to day 60. The subcutaneous tumour formation volume of the mice in the $\lg G$ + adenovirus group was the largest and the growth rate the fastest; the subcutaneous tumour formation volume of the mice in the $\lg G$ + adenovirus group. The subcutaneous tumour formation volume of the mice in the 606862 + adenovirus group was reduced, and the growth rate was further slowed compared with that of the first two groups. In the four groups, mice in the 606862 + adenovirus group, and the tumour growth rate as well as the tumour formation volume were second only to those in the 606862 + adenovirus group. In contrast, CD206-induced tumour growth was inhibited after treatment with 606862, so the tumour growth rate as well as the tumour formation volume in mice in the 606862 group were significantly higher than those in the mice treated with 606862 (Fig. 3A, B). Finally, the subcutaneous tumour formation volume of the mice in the 606862 group was the smallest and the growth rate the slowest. The differences were statistically significant (p < 0.05).

At the end-point of the observation, the subcutaneous tumour tissues were isolated and weighed, with the heaviest tumour weight after euthanasia in the IgG+adenovirus group and the lightest in the C068C2 group. In the other two groups,



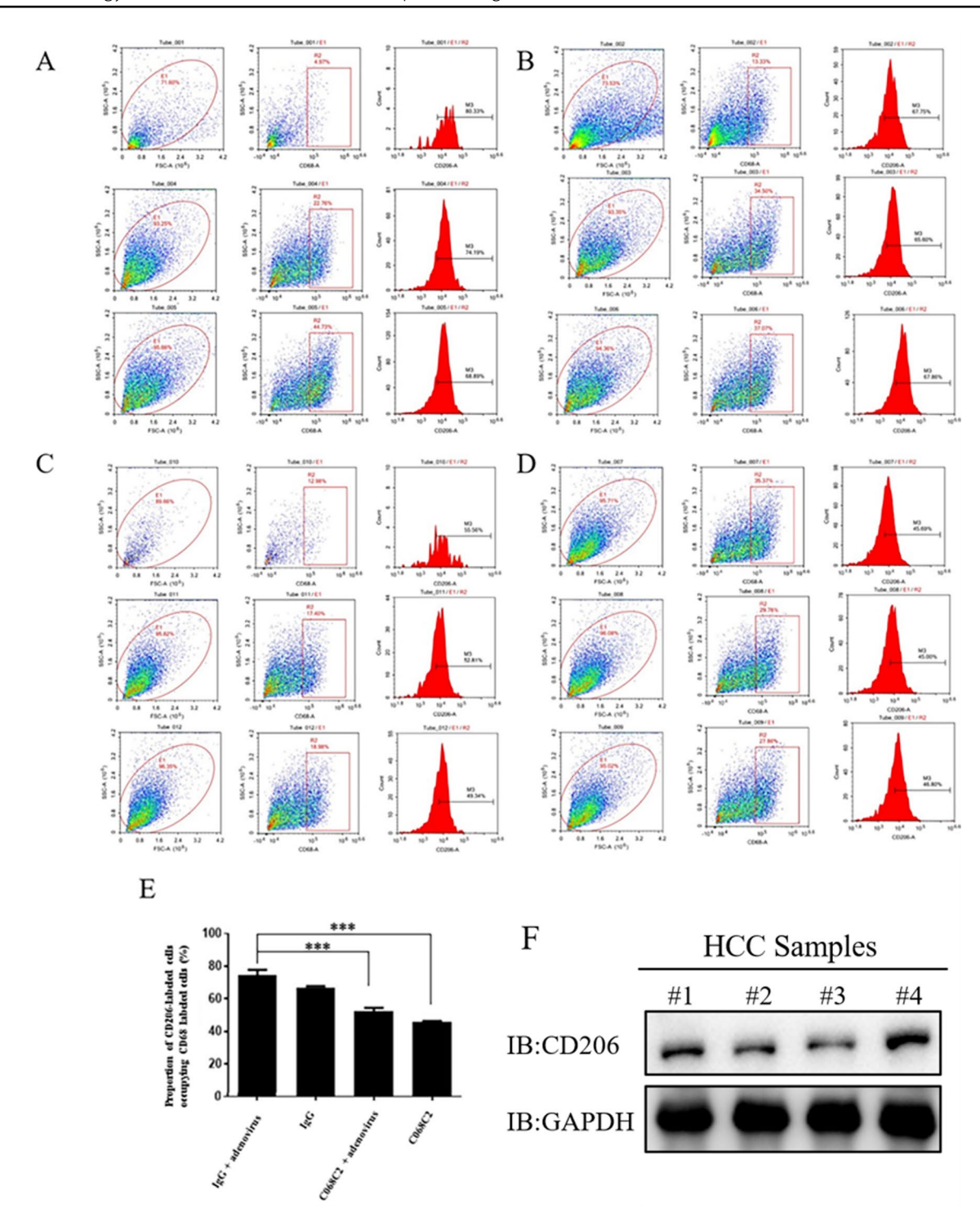


Fig. 1 Differences in CD206 expression levels in tumour tissues by flow cytometry. A-E The proportion of CD206 labeled cells occupying CD68 labeled cells in each group. A IgG+a denovirus group. B IgG group. C IgG+a denovirus group. D IgG+a group. D

the tumour weight after euthanasia was intermediate between the weights of these two groups, with a statistically significant difference in tumour tissue weight (p < 0.001). The results showed that the mice in the lgG + adenovirus group with CD206



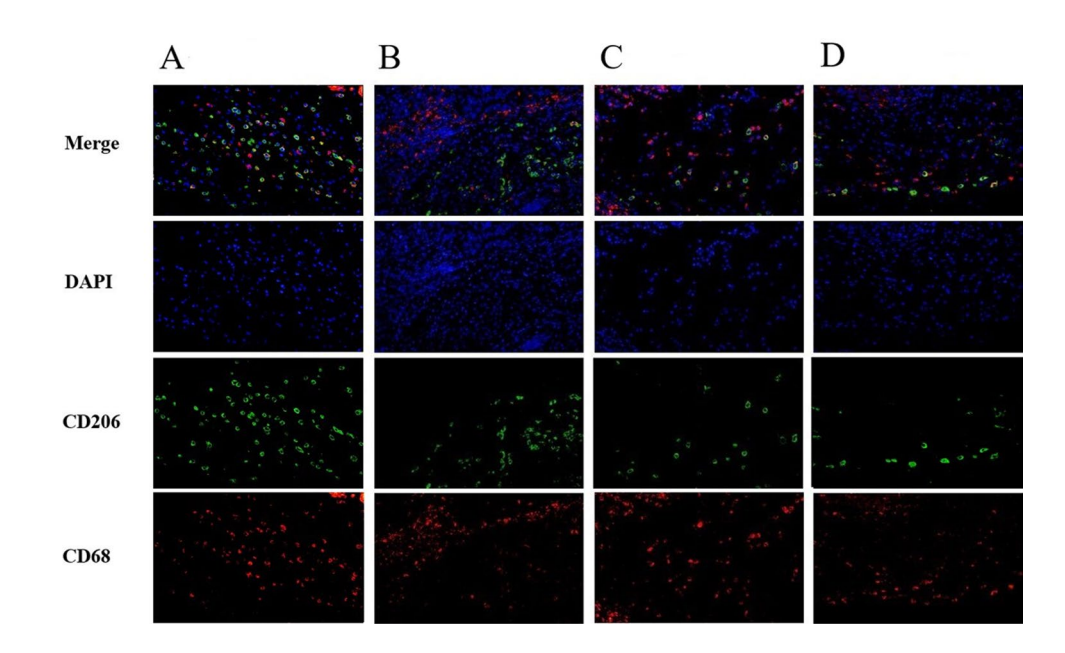
Table 2 Differences in CD206 detected by immunofluorescence between the groups

Group	Expression profile		$\chi^{2 a}$	<i>p</i> value ^a	<i>p</i> value ^b
	Low expres- sion	High expres- sion			
lgG + adenovirus group	0	5	15.791	0.001	
lgG group	2	3			0.444
C068C2 + adenovirus group	4	1			0.048
C068C2 group	5	0			800.0

n=5 per group

b: Further two-by-two comparisons between groups were performed using the Bonferroni test. The data in the IgG+adenovirus group was compared with the data in the three groups of IgG group, C068C2 + adenovirus group and C068C2 group in pairs, respectively

Fig. 2 Different expression levels of CD206 in tumour tissues detected by immunofluorescence staning. A IgG + adenovirus group. B IgG group. C C068C2+adenovirus group. **D** C068C2 group. Magnification, ×100; scale bar, 200 um



overexpression had the largest tumour volume and the fastest tumour growth rate, and the tumour-bearing mice had the heaviest tumour weight after euthanasia (Fig. 3).

3.4 Effect of different expression levels of CD206 on tumour cell apoptosis

To understand the mechanism of TAMs of different phenotypes on HCC cells, TUNEL staining was used to analyse the apoptosis of HCC cells. Compared with the mice in the IgG+adenovirus group, the mice in the C068C2+adenovirus group and C068C2 group had a significantly reduced number of TUNEL-positive cells, respectively, (p < 0.01 for both groups; Table 3, Fig. 4A-E), indicating that the apoptosis rate was significantly higher in the IgG+adenovirus group than in the C068C2+adenovirus group and C068C2 group.

This suggests that M2-type TAMs dominated in the IgG+adenovirus group, which stimulated the fast growth of liver cancer cells. When a tumour grows too fast, the blood and nutrient supplies are insufficient for tumour growth, resulting in necrosis in the tumour centre, which manifests as the apoptosis of tumour cells. CD206 was inhibited in the tumour tissue of the C068C2 group, and the proportion of M2-type TAMs was decreased in liver cancer tissues.



a:The four-group data were analyzed using χ^2 test

Fig. 3 Effect of different expression levels of CD206 on tumour volume and growth.

A Representative pictures of subcutaneous tumour formation in mice in each group. B Change curve of subcutaneous tumour volume in tumour -bearing mice of each group.

C Tumour weight of tumour -bearing mice in each group after sacrifice. (*:P < 0.05;**: P < 0.01;***: P < 0.001)

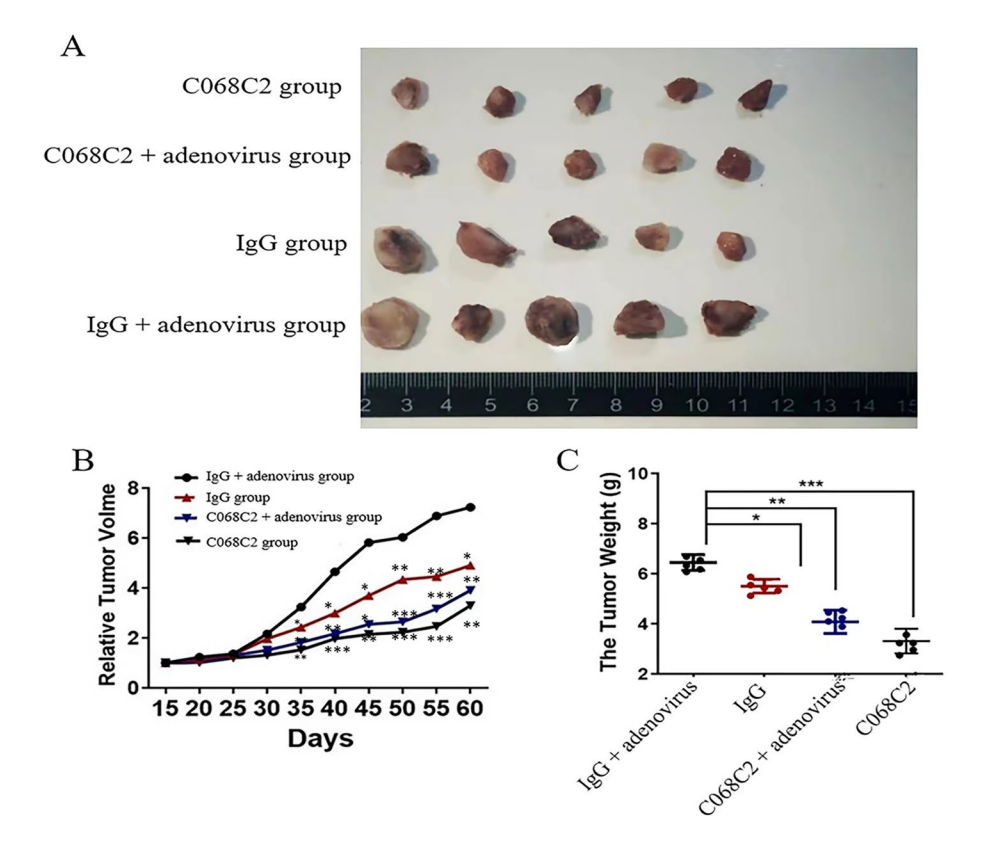


Table 3 Difference in apoptosis rate of tumor cells detected by TUNEL staining

Group	Apoptosis rate		χ2a	p value ^a	<i>p</i> value ^b
	Low	High			
lgG+adenovirus	0	5	22.522	< 0.001	
IgG	1	4			1.000
C068C2+adenovirus	5	0			0.008
C068C2	5	0			0.008

n=5 per group

b: Further two-by-two comparisons between groups were performed using the Bonferroni test. The data in the IgG+adenovirus group was compared with the data in the three groups of IgG group, C068C2+adenovirus group and C068C2 group in pairs, respectively

3.5 Effect of different expression levels of CD206 on the concentration of inflammatory factors in serum and tumour tissues

The levels of the inflammatory factor TGF- β in the serum and tumour tissues of the tumour-bearing mice in each group were detected by ELISA. Comparison among the four groups showed that the concentration of TGF- β was the highest in the IgG+adenovirus group, both in the serum and tumour tissues of the mice; the difference was statistically significant (p < 0.01). The levels of IL-6 in the serum and tumour tissues of the tumour-bearing mice in each group were detected using ELISA. The results were consistent with those of TGF- β detection, and the differences were also statistically significant (p < 0.01; Fig. 5A–D).



a:The four-group data were analyzed using χ^2 test

Fig. 4 Effect of different CD206 expression levels on tumour cell apoptosis by TUNEL fluorescence staining. **A-D** TUNEL fluorescence staining of apoptosis in each group. A IgG+adenovirus group. B IgG group. C C068C2 + adenovirus group. D C068C2 group. (Magnification, × 100; scale bar, 200 um). **E** Apoptosis rate of TUNEL results between the four groups were presented in graph. (Mean ± SE; ***: P < 0.001)

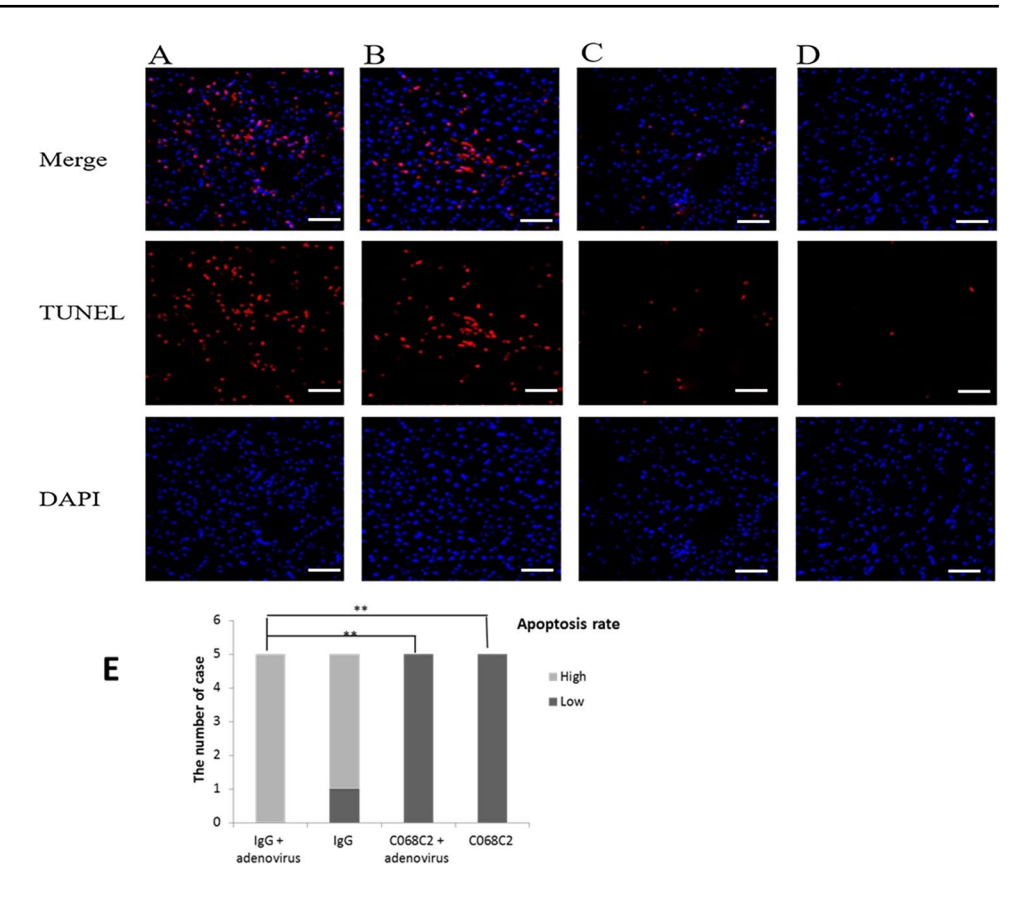
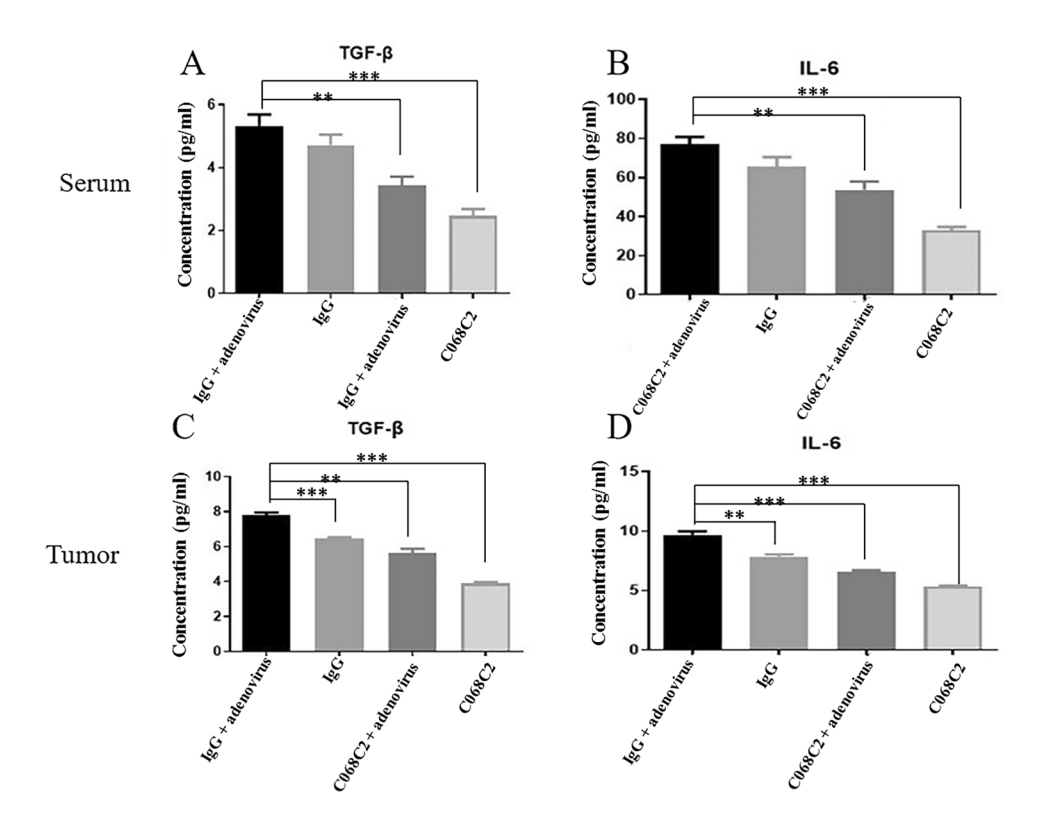


Fig. 5 The effect of different expression levels of CD206 on the concentration of inflammatory factors in serum and tumour tissues by Elisa assay. **A** TGF-β concentration in serum of each group. B IL-6 concentration in serum of each group. \boldsymbol{C} TGF- $\boldsymbol{\beta}$ concentration in tumour tissues of each group. D IL-6 concentrations in tumour tissues of each group. The four-group data was analyzed using one-way ANOVA and further two-bytwo comparisons between groups were performed using the LSD-t test. (Mean ± SE; **: P < 0.01;***: P < 0.001)





4 Discussion

Hepatocellular carcinoma is one of the most malignant tumours worldwide, and its morbidity and mortality are increasing annually. According to the current study, the aetiology of some HCCs has been clarified, but the mechanism is not yet clear [18]. Cirrhosis caused by chronic viral hepatitis, which in turn develops into HCC, is the main factor in the pathogenesis of liver cancer, and HCC is one of the malignant tumours closely related to inflammation [19].

Tumour-associated macrophages, a type of cell present in the TME, are divided into M1-type TAMs and M2-type TAMs. M1-type TAMs can play a role in inhibiting tumours, mainly from two perspectives: directly mediated cytotoxicity and antibody-dependent cell-mediated cytotoxicity. The directly mediated cytotoxic effect is that M1-type TAMs can release molecules that have toxic effects on tumour cells, such as reactive oxygen species and nitric oxide, and then kill those tumour cells, but this process of releasing killing molecules is slow [20]. On the other hand, M2-type TAMs play a role in promoting tumours, mainly by promoting the proliferation of tumour cells, tumour growth, tumour metastasis and the formation of tumour micro-vessels and lymphatic vessels; the above effects are exerted mainly by inhibiting T-lymphocyte-mediated anti-tumour immune responses [21–23]. M1-type and M2-type TAMs represent dynamic changes in the TME and can transform into each other by changing the TME, thereby affecting the polarisation of TAMs.

This study found that both M1-type and M2-type TAMs were present in tumour tissue and that the higher the number of M2-type TAMs, the faster the tumour growth, suggesting a higher degree of tumour malignancy. However, the higher the number of M1-type TAMs, the more limited the tumour growth rate, which was also consistent with the characteristics of M1-type and M2-type TAMs. At the same time, it has also been confirmed in previous studies that the higher the number of M2-type TAMs, the worse the overall prognosis of the tumour [24–26], with a poor prognosis predicting the proliferation of tumour cells, fast growth and metastasis. This is consistent with the findings of the current study.

Studies have shown that the expression of CD206 is related to the differentiation, depth of invasion, vascular tumour thrombus and nerve invasion of colon cancer. The higher the expression of CD206, the lower the differentiation, the deeper the depth of invasion and the more likely vascular tumour thrombus and nerve invasion of colon cancer. The above factors are also the influencing factors of low disease-free survival and overall survival (OS), suggesting that a high expression of CD206 has a relatively bad prognosis [27].

In related studies on lung cancer, lung cancer cells induced TAMs to polarise to M2-type TAMs with positive CD206 expression via THP-1 and stimulate the production of a variety of cytokines, which, in turn, promoted tumour development [14]. In a study on ovarian cancer, although the density of CD206-positive TAMs was not a prognostic factor in patients with ovarian cancer, an increased proportion of CD206-positive cells was found to reflect lower PFS and OS [28]. At the same time, CD206-positive TAMs were found to have high levels of oncogenic cytokine expression in the ascites of patients with ovarian cancer using transcriptome sequencing technology, which in turn promoted tumour development [29].

The present study found that among the mice, CD206-overexpressing hepatocarcinoma-bearing mice had a larger tumour size and faster tumour growth rate, and the tumour-bearing mice had a heavier tumour weight after euthanasia. Conversely, the hepatocarcinoma-bearing mice that inhibited CD206 expression had the smallest tumour size and the slowest tumour growth rate, and the tumour-bearing mice had the lightest tumour weight after euthanasia. The results of this study are consistent with the above findings.

The relationship between tumours and inflammation has been of wide concern and has also developed greatly, with the correlation between the two a hot topic and the focus of current research. Lin X et al. reported that immune-related genes in HCC are significantly associated with both tumour-infiltrating immune cells and disease prognosis [30]. Peng B et al. reported that the CIBERSORTx, TIMER2.0 and GEPIA2 tools were employed to explore the relation-ship between the prognostic signature and immune cell infiltration, and they established a six-gene signature as a reliable model with significant therapeutic possibility for prognosis and OS estimation in patients with HCC [31]. Many epidemiological studies have found that the occurrence and development of human tumours are directly related to chronic inflammation caused by infectious factors, such as bacteria and viruses [32–34]. Transforming growth factor- β belongs to the TGF- β superfamily and is mainly studied in terms of inflammation and other aspects. With the continuous deepening of research, TGF- β has also been found to play an important role in the regulation of cell growth, differentiation and immune function [35–37]. Colorectal cancer cells have been reported to use TGF- β through collagen triple-helix repeat containing 1 (CTHRC1) to regulate TAM polarisation to the M2 type, promote



the growth of tumour cells and increase the number of liver metastases from colon cancer. At this time, the use of the CTHRC1 antibody to inhibit TGF- β in TAMs while blocking PD-1/PD-L1 can effectively reduce the number of colorectal liver metastases [38]. In non-small-cell lung cancer (NSCLC), the M2 type of TAM is predominant. This type can increase the expression of SOX9 and activate epithelial–mesenchymal transition by secreting TGF- β , which can promote the development, invasion and metastasis of NSCLC [39].

Interleukin-6 is a cytokine produced by a variety of cells that produces extensive and pleiotropic effects on a range of different cells. Interleukin-6 plays an important role in immune regulation, immune response, stress response and anti-infection; additionally, it can effectively regulate both the inflammatory response and the growth and differentiation of a variety of cells, especially in tumour production, where IL-6 is produced in large amounts [40–42]. The mechanism of IL-6 in promoting tumour progression is different from that of TGF- β , and its correlation with TAMs is by acting through different signalling pathways than those of TGF- β , thereby laying a theoretical foundation for targeted TAM therapy for liver cancer.

The present study also found that IL-6 levels in peripheral serum and tumour tissue were similarly increased in hepatocarcinoma-bearing mice with a high expression of M2-type TAMs; IL-6 levels in peripheral serum and tumour tissue were lowest in hepatocarcinoma-bearing mice with inhibition of M2-type TAMs. M2-like TAMs secreted more IL-6 under the combined action of hepatocarcinoma cells and extracellular matrix, which in turn induced the production of inflammation in the hepatocarcinoma TME, activated inflammation-related signalling pathways, further stimulated epithelial–mesenchymal transition, promoted the proliferation of HCC cells and promoted the growth and progression of HCC. Therefore, it can be inferred that IL-6 can affect the expression of M2-type TAMs. Furthermore, M2-type TAMs can also affect the level of IL-6.

In summary, differences in the size of mouse tumour formation were correlated with CD206 expression during the construction of viral and mouse HCC xenograft models, and different polarisation states of TAMs were also correlated with tumour growth. Therefore, this study further validated CD206 as a specific marker of M2-type TAMs. The role in promoting tumour growth, invasion and metastasis was further clarified by detecting the expression of different numbers of M2-type TAMs.

This study has some limitations. First, it did not detect the levels of CD4+ and CD8+T lymphocytes involved in affecting the immune function of the body and exerting the immune escape mechanism. Whether the two change correspondingly with the classification and content of TAMs is unclear. Second, whether the overexpression of CD206 can functionally convert TAMs into M2-type TAMs remains to be investigated. Finally, the relationship between M2-type TAMs and inflammatory factors is unknown.

5 Conclusion

The present study found that CD206 overexpression accelerated the progression of HCC and changed the tumour immune microenvironment. The high expression level of CD206 in HCC increased the M2-type polarisation of TAMs and induced the expression of TGF- β and IL-6 in tumour tissues and serum, thereby promoting HCC progression.

Acknowledgements Not applicable.

Author contributions Conception and design of the work: Mao ZY, Han YL; Data collection: Mao ZY, Han YL, Lin YL, Bai L; Supervision: Mao ZY, Han YL; Analysis and interpretation of the data: Lin YL, Bai L; Statistical analysis: Mao ZY, Han YL; Drafting the manuscript: Mao ZY, Han YL; Critical revision of the manuscript: Mao ZY, Han YL, Lin YL, Bai L; Approval of the final manuscript: Mao ZY, Han YL, Lin YL, Bai L.

Funding The authors have received no financial support for the research, authorship, or publication of this manuscript.

Data availability All data generated or analyzed during this study are included in this published article.

Declarations

Ethics approval and consent to participate This study was conducted in accordance with the Declaration of Helsinki and approved by the Ethics Committee of the First Medical Center, Chinese PLA General Hospital.

Statement of the maximal tumor size/burden According to the criteria set by the Hospital Ethics Committee based on the Guidelines for Humane Endpoint Review of Animal Experiments in China, the tumor length on the back of mice should be less than 17 mm.



In this study, the size of the tumour was measured with Vernier callipers, and the length (L) and width (W) of the tumour were recorded. The volume (V) was calculated as: $(L \times W^2) \times 0.5$. In this study, all tumors did not exceed 15 mm in length and 1 cm³ in volume, which meets the requirement for maximal tumor burden.

Consent for publication Not applicable.

Competing interests The authors declare no competing interests.

Open Access This article is licensed under a Creative Commons Attribution-NonCommercial-NoDerivatives 4.0 International License, which permits any non-commercial use, sharing, distribution and reproduction in any medium or format, as long as you give appropriate credit to the original author(s) and the source, provide a link to the Creative Commons licence, and indicate if you modified the licensed material. You do not have permission under this licence to share adapted material derived from this article or parts of it. The images or other third party material in this article are included in the article's Creative Commons licence, unless indicated otherwise in a credit line to the material. If material is not included in the article's Creative Commons licence and your intended use is not permitted by statutory regulation or exceeds the permitted use, you will need to obtain permission directly from the copyright holder. To view a copy of this licence, visit http://creativecommons.org/licenses/by-nc-nd/4.0/.

References

- 1. Kudo M. Urgent global need for PIVKA-II and AFP-L3 measurements for surveillance and management of hepatocellular carcinoma. Liver Cancer. 2024;13(2):113–8.
- 2. Wang Y, Yang Y, Zhao Z, Sun H, Luo D, Huttad L, et al. A new nomogram model for prognosis of hepatocellular carcinoma based on novel gene signature that regulates cross-talk between immune and tumor cells. BMC Cancer. 2022;22(1):379.
- 3. Chidambaranathan-Reghupaty S, Fisher PB, Sarkar D. Hepatocellular carcinoma (HCC): epidemiology, etiology and molecular classification. Adv Cancer Res. 2021;149:1–61.
- 4. Arneth B. Tumor microenvironment. Medicina (Kaunas). 2019:56(1):15.
- 5. Zhang Y, Qin N, Wang X, Liang R, Liu Q, Geng R, et al. Glycogen metabolism-mediated intercellular communication in the tumor micro-environment influences liver cancer prognosis. Oncol Res. 2024;32(3):563–76.
- 6. Hinshaw DC, Shevde LA. The tumor microenvironment innately modulates cancer progression. Cancer Res. 2019;79(18):4557–66.
- He M, Zhang M, Xu T, Xue S, Li D, Zhao Y, et al. Enhancing photodynamic immunotherapy by reprograming the immunosuppressive tumor microenvironment with hypoxia relief. J Control Release. 2024;368:233–50.
- 8. Liu MQ, Bao CJ, Liang XF, Ji XY, Zhao LQ, Yao AN, et al. Specific molecular weight of *Lycium barbarum* polysaccharide for robust breast cancer regression by repolarizing tumor-associated macrophages. Int J Biol Macromol. 2024;261(Pt 1): 129674.
- 9. Wildes TJ, Dyson KA, Francis C, Wummer B, Yang C, Yegorov O, et al. Immune escape after adoptive T-cell therapy for malignant gliomas. Clin Cancer Res. 2020;26(21):5689–700.
- 10. Erin N, Grahovac J, Brozovic A, Efferth T. Tumor microenvironment and epithelial mesenchymal transition as targets to overcome tumor multidrug resistance. Drug Resist Updat. 2020;53: 100715.
- 11. Pan Y, Yu Y, Wang X, Zhang T. Tumor-associated macrophages in tumor immunity. Front Immunol. 2020;3(11): 583084.
- 12. Wang X, Li D, Li G, Chen J, Yang Y, Bian L, et al. Enhanced therapeutic potential of hybrid exosomes loaded with paclitaxel for cancer therapy. Int J Mol Sci. 2024;25(7):3645.
- 13. Wang X, Zhang L, Zhou Y, Wang Y, Wang X, Zhang Y, et al. Chronic Stress exacerbates the immunosuppressive microenvironment and progression of gliomas by reducing secretion of CCL3. Cancer Immunol Res. 2024;12(5):516–29.
- 14. Guo Z, Song J, Hao J, Zhao H, Du X, Li E, et al. M2 macrophages promote NSCLC metastasis by upregulating CRYAB. Cell Death Dis. 2019:10(6):377.
- 15. Bejarano L, Jordão MJC, Joyce JA. Therapeutic targeting of the tumor microenvironment. Cancer Discov. 2021;11(4):933-59.
- 16. Gordon S, Plüddemann A. Tissue macrophages: heterogeneity and functions. BMC Biol. 2017;15(1):53.
- 17. Barbati C, Bromuro C, Vendetti S, Torosantucci A, Cauda R, Cassone A, et al. The glycan ectodomain of SARS-CoV-2 spike protein modulates cytokine production and expression of CD206 mannose receptor in PBMC cultures of pre-COVID-19 healthy subjects. Viruses. 2024;16(4):497.
- 18. Lino-Silva LS, Lajous M, Brochier M, Santiago-Ruiz L, Melchor-Ruan J, Xie Y, et al. Aflatoxin levels and prevalence of TP53 aflatoxin-mutations in hepatocellular carcinomas in Mexico. Salud Publica Mex. 2022;64(1):35–40.
- 19. Yang YM, Kim SY, Seki E. Inflammation and liver cancer: molecular mechanisms and therapeutic targets. Semin Liver Dis. 2019;39(1):26-42.
- 20. Yoon J, Le XT, Kim J, Lee H, Nguyen NT, Lee WT, et al. Macrophage-reprogramming upconverting nanoparticles for enhanced TAM-mediated antitumor therapy of hypoxic breast cancer. J Control Release. 2023;360:482–95.
- 21. Qiu Y, Lu G, Li N, Hu Y, Tan H, Jiang C. Exosome-mediated communication between gastric cancer cells and macrophages: implications for tumor microenvironment. Front Immunol. 2024;15:1327281.
- 22. Zhou M, Yu H, Bai M, Lu S, Wang C, Ke S, et al. IRG1 restrains M2 macrophage polarization and suppresses intrahepatic cholangiocarcinoma progression via the CCL18/STAT3 pathway. Cancer Sci. 2024;115(3):777–90.
- 23. Chiang Y, Lu LF, Tsai CL, Tsai YC, Wang CC, Hsueh FJ, et al. C-C chemokine receptor 4 (CCR4)-positive regulatory T cells interact with tumor-associated macrophages to facilitate metastatic potential after radiation. Eur J Cancer. 2024;198: 113521.
- Huang X, He C, Lin G, Lu L, Xing K, Hua X, et al. Induced CD10 expression during monocyte-to-macrophage differentiation identifies a unique subset of macrophages in pancreatic ductal adenocarcinoma. Biochem Biophys Res Commun. 2020;524(4):1064–71.



- 25. Zhang X, Chen L, Dang WQ, Cao MF, Xiao JF, Lv SQ, et al. CCL8 secreted by tumor-associated macrophages promotes invasion and stemness of glioblastoma cells via ERK1/2 signaling. Lab Invest. 2020;100(4):619-29.
- 26. Wu H, Zhang X, Han D, Cao J, Tian J. Tumour-associated macrophages mediate the invasion and metastasis of bladder cancer cells through CXCL8. PeerJ. 2020;8: e8721.
- 27. Feng Q, Chang W, Mao Y, He G, Zheng P, Tang W, et al. Tumor-associated macrophages as prognostic and predictive biomarkers for postoperative adjuvant chemotherapy in patients with stage II colon cancer. Clin Cancer Res. 2019;25(13):3896-907.
- 28. Li H, Miao YQ, Suo LP, Wang X, Mao YQ, Zhang XH, et al. CD206 modulates the role of M2 macrophages in the origin of metastatic tumors. J Cancer. 2024;15(5):1462-86.
- 29. Zheng D, Long S, Xi M. Identification of TRPM2 as a potential therapeutic target associated with immune infiltration: a comprehensive pan-cancer analysis and experimental verification in ovarian cancer. Int J Mol Sci. 2023;24(15):11912.
- 30. Lin X, Tian C, Pan F, Wang R. A novel immune-associated prognostic signature based on the immune cell infiltration analysis for hepatocellular carcinoma. Oncologie. 2024;26(1):91-103.
- 31. Peng B, Ge Y, Yin G. A novel prognostic gene signature, nomogram and immune landscape based on tanshinone IIA drug targets for hepatocellular carcinoma: comprehensive bioinformatics analysis and in vitro experiments. Biocell. 2023;47(7):1519-35.
- 32. Singh N, Baby D, Rajguru JP, Patil PB, Thakkannavar SS, Pujari VB. Inflammation and cancer. Ann Afr Med. 2019;18(3):121-6.
- Lin WP, Li H, Sun ZJ. T cell exhaustion initiates tertiary lymphoid structures and turbocharges cancer-immunity cycle. EBioMedicine. 2024;104: 105154.
- 34. Guerra F, Ponziani FR, Cardone F, Bucci C, Marzetti E, Picca A. Mitochondria-derived vesicles, sterile inflammation, and pyroptosis in liver cancer: partners in crime or innocent bystanders? Int J Mol Sci. 2024;25(9):4783.
- 35. Wang H, Yung MMH, Ngan HYS, Chan KKL, Chan DW. The impact of the tumor microenvironment on macrophage polarization in cancer metastatic progression. Int J Mol Sci. 2021;22(12):6560.
- 36. Liu C, Zhang W, Wang J, Si T, Xing W. Tumor-associated macrophage-derived transforming growth factor-ß promotes colorectal cancer progression through HIF1-TRIB3 signaling. Cancer Sci. 2021;112(10):4198–207.
- 37. You S, Han X, Xu Y, Sui L, Song K, Yao Q. High expression of SLC7A1 in high-grade serous ovarian cancer promotes tumor progression and is involved in MAPK/ERK pathway and EMT. Cancer Med. 2024;13(10): e7217.
- 38. Zhang XL, Hu LP, Yang Q, Qin WT, Wang X, Xu CJ, et al. CTHRC1 promotes liver metastasis by reshaping infiltrated macrophages through physical interactions with TGF-β receptors in colorectal cancer. Oncogene. 2021;40(23):3959–73.
- Barbosa S, Laureano NK, Hadiwikarta WW, Visioli F, Bonrouhi M, Pajdzik K, et al. The role of SOX2 and SOX9 in radioresistance and tumor recurrence. Cancers (Basel). 2024:16(2):439.
- 40. Sørensen MD, Kristensen BW. Tumour-associated CD204+ microglia/macrophages accumulate in perivascular and perinecrotic niches and correlate with an interleukin-6-enriched inflammatory profile in glioblastoma. Neuropathol Appl Neurobiol. 2022;48(2): e12772.
- 41. Neo SY, Tong L, Chong J, Liu Y, Jing X, Oliveira MMS, et al. Tumor-associated NK cells drive MDSC-mediated tumor immune tolerance through the IL-6/STAT3 axis. Sci Transl Med. 2024;16(747):eadi2952.
- 42. Zhang L, Bonomi PD. Immune system disorder and cancer-associated cachexia. Cancers (Basel). 2024;16(9):1709.

Publisher's Note Springer Nature remains neutral with regard to jurisdictional claims in published maps and institutional affiliations.

